

# IMPLEMENTATION OF HOLLOW ELECTRON LENSES IN SixTrack AND FIRST SIMULATION RESULTS FOR THE HL-LHC<sup>\*†</sup>

M. Fitterer<sup>‡</sup>, G. Stancari, A. Valishev, Fermilab, Batavia, IL 60510, USA

R. De Maria, S. Redaelli, K. Sjobak, J. F. Wagner<sup>1§</sup>

CERN, Geneva, Switzerland

<sup>1</sup>Goethe University, Frankfurt, Germany

## Abstract

Electron lenses have found a wide range of applications for hadron colliders, where the main applications are machine protection and beam-beam compensation. This paper summarizes the status of the current electron lens implementation in SixTrack with the focus on hollow electron beams for beam collimation and shows some first simulation results of the High-Luminosity upgrade of the LHC (HL-LHC).

## INTRODUCTION

SixTrack is a 6D symplectic single-particle tracking code [1] used for studying the dynamic aperture and the collimation system of high-energy circular machines like the LHC, FCC and recently the SPS. Besides other major code developments [2], a new tracking module for electron lenses (e-lenses) has been added that provides a flexible interface for various applications of e-lenses to be succeeded by the implementation of the corresponding maps. This implementation now in the main branch of the code replaces a previous implementation of the hollow electron lens (HEL) [3] with the following major improvements:

- implementation of a new e-lens input block providing the framework for the different applications,
- implementation of the HEL as standard element instead of previously a collimator in the collimation version of SixTrack. This explicitly now allows to also use all the non-linear tracking and analysis tools within SixTrack which are by default not available in the collimation version.

In the following sections we will give a more detailed description of this implementation, as well as a short overview of e-lenses with emphasis on halo control with hollow e-beams followed by first simulation results for HL-LHC.

## PRINCIPLE OF ELECTRON LENSES AND IMPLEMENTATION IN SIXTRACK

As electron lenses one in general denotes a low energy electron beam, which interacts with the hadron beam, while the two beams are sharing the same aperture. The e-beam is generated with an electron gun. The e-beam is then guided



Figure 1: Layout of the HL-LHC HEL exemplary for the general layout of e-lenses [4].

and at the same time confined with strong solenoids in order to travel co-axial to the hadron aperture to be finally dumped on a collector (see Fig. 1). The shape of the generated e-beam is mainly determined by the cathode of the gun, which allows the generation of e-beams with very diverse distributions. In turn, the shape of the e-beam distribution as well as its distance to the hadron beam defines the generated electromagnetic field, opening the door to a multiplicity of applications like head-on and long-range beam-beam compensation, and halo control and cleaning [5]. In order to provide a common interface for the different application corresponding to different maps in the code, a new input block for e-lenses has been added with the general structure [6]:

### ELEN

**name profile parameters**

where **name** is the name of the element, **profile** is the distribution of the e-beam, e.g. annular for the HEL, and **parameters** are the parameters of the map of the corresponding profile, i.e. the maximum kick angle and inner and outer radius for the HEL. Based on the selected profile the corresponding map is then used within the code. Currently, only the map of a uniform hollow e-beam distribution as considered for halo control in the HL-LHC has been implemented; to be followed by the maps for other applications.

## HOLLOW BEAM COLLIMATION AND IMPLEMENTATION IN SIXTRACK

The concept of hollow e-beams for halo control in the LHC is illustrated in Fig. 2. In this case the e-lens has the function of generating a non-linear kick on the halo particles while leaving the core of the beam unperturbed. Due to the non-linear kick, halo particles diffuse faster and can then be intercepted in a controlled way by the collimation system. For this purpose, an annular uniform distribution with inner radius  $R_1$  and outer radius  $R_2$  is best suited. The distribution together with the radial kick is illustrated in Fig. 3.

<sup>\*</sup> Fermilab is operated by Fermi Research Alliance, LLC, under Contract DE-AC02-07CH11359 with the US Department of Energy.

<sup>†</sup> Research supported by the High Luminosity LHC project.

<sup>‡</sup> mfittere@fnal.gov

<sup>§</sup> joschka.wagner@cern.ch

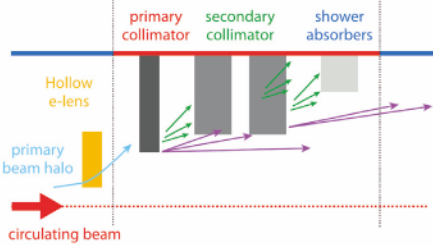


Figure 2: The hollow electron lens (HEL) as a complementary device for the present collimation system, actively controlling the primary beam halo.

The kick can be described analytically by a shape function  $f(r)$  and a maximum kick strength  $\theta_{\max}$ :

$$\theta(r) = \frac{f(r)}{(r/R_2)} \cdot \theta_{\max} \cdot \frac{1}{1 + \delta},$$

with  $r = \sqrt{x^2 + y^2}$  and  $\delta$  the relative momentum deviation. The shape function  $f(r)$  is given by:

$$f(r) = \begin{cases} 0 & , \quad r \leq R_1, \\ \frac{r^2 - R_1^2}{R_2^2 - R_1^2} & , \quad R_1 < r < R_2, \\ 1 & , \quad r \geq R_2, \end{cases}$$

and the maximum  $r$ -independent kick angle by:

$$\theta_{\max} = \frac{2LI_T(1 \pm \beta_e\beta_p)}{4\pi\epsilon_0(B\rho)_p\beta_e\beta_pc^2} \cdot \frac{1}{R_2},$$

where  $L$  is the length of the HEL,  $I_T$  the total e-beam current,  $\beta_e$  and  $\beta_p$  the relativistic  $\beta$  of electron and proton beam,  $B\rho$  the magnetic rigidity of the protons,  $c$  the speed of light and  $\epsilon_0$  the vacuum permittivity. The  $\pm$ -sign represents the two cases of the e-beam traveling in the direction of the proton beam (“-”) or in the opposite direction (“+”) as it is the case for hollow beam collimation. In addition, theoretical models have been developed to describe the effect of the bends of the HEL [7] and also for non-ideal profiles [8]. It is planned to review and further extend these two options and implement them in SixTrack. These extensions will be particularly relevant to study the effect of the HEL on the beam core as for the ideal profile, the field vanishes while in

the case of the bends and profile imperfections the field at the center of the beam is non-zero [9].

Beside a continuous direct e-beam current (DC) the HEL can also be operated in pulsed mode or the voltage (and thus current) of the e-beam current can be modulated. These additional modes of operation are considered in order to further increase the diffusion rate of the halo particles if needed by applying noise. Using the DYNAMIC Kicks module (DYNK) of SixTrack [10], which allows for time-dependent modification of beam line elements, different modes of the e-lens can easily be added. Explicitly, the following modes have been implemented:

- **stochastic-amplitude:** an additional random uniform voltage modulation is added to the DC current,
- **stochastic-ONOFF:** the voltage is randomly turned ON or OFF every turn with a probability between 0 and 1 to be ON.
- **resonant-tune:** the voltage is changed according to a sinusoidal function with the same frequency as the machine tune.
- **resonant-turn:** switched ON only every  $n^{\text{th}}$  turn.

## HOLLOW ELECTRON LENS STUDIES FOR HL-LHC

In the current LHC, the beam halo is only controlled passively by intercepting halo particles with the collimation system. A recent review however showed, that to reach the full performance of the HL-LHC an active control of the halo is needed and that the HEL is considered the superior technology compared to other available methods (see [11]). To evaluate the performance of the HEL, a simulation campaign has been started using the simulation codes SixTrack and Lifetrac for comparison [12] including also a comparison of the two codes.

### Simulation Parameters

In previous simulations it has been shown that the halo removal rates in general increase with the strength of the machine non-linearities [13]. As beam-beam represents the strongest non-linearity in the HL-LHC and the non-linearities due to magnet errors are larger at injection, the smallest halo diffusion rate and thus the worst case scenario is to be expected for separated beams before the squeeze, which has been chosen as base scenario for the simulations presented in this paper. As HL-LHC layout the version V1.0 has been used with the HEL installed at -40 m from IP4, which is favorable as it provides equal  $\beta$ -functions in both planes and thus an optimal overlap of the hollow e-beam with the proton beam. The collimation system is represented by the three primary collimators (TCP) – horizontal, vertical and skew – as black absorbers. No magnet and misalignment errors have been taken into account. A list of all relevant machine and beam parameters is given in Table 1 and the collimator settings together with the HEL and proton beam distribution are illustrated in Fig. 3. The observable used for the halo removal rate in this paper is the relative particle

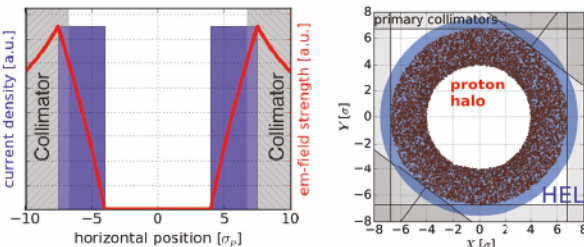


Figure 3: Sketch of the kick from a uniform hollow e-beam distribution (left) and halo input distribution with overlaying HEL beam and collimator positions as used in the HL-LHC simulations (right).

Table 1: Simulation Parameters

HL-LHC proton beam	Value	Unit
$\beta^*$ at IP1/5	6	m
collimator opening (TCP)	6.74	$\sigma_p$
beam Energy $E_p$	7	TeV
normalized beam emittance $\epsilon_{N,p}$	2.5	$\mu\text{m}$
inner/outer radius (transv. distr.)	4/6.74	$\sigma_p$
bunch length	7.55	cm
hollow electron lens	Value	Unit
length $L$	3	m
beam Energy $E_e$	10	keV
inner/outer radius $R_1/R_2$	4/7.53	$\sigma_p$

loss as a function of the turn number  $t^1$ :

$$I_{\text{rel}}(t) = \frac{(N(t) - N(t = 10000))}{N(t = 10000)} \quad (1)$$

assuming a uniform hollow transverse distribution in beam radius  $r$  and Gaussian distribution in the longitudinal plane with  $10^4$  particles has been tracked for  $10^6$  turns. To obtain life time estimates, these values would have to be combined with a folding of the beam distribution and the tracked distribution.

### Code Comparison of SixTrack and Lifetrac

For a first benchmarking of the two simulation codes, the DC and stochastic-amplitude mode have been simulated for different chromaticities  $Q'_{x,y}$  and octupole currents  $I_{\text{oct}}$  and an e-beam current of  $I_e = 5$  A leading to  $\theta_{\max} = 371$  nrad. The halo removal rates as defined in Eq. 1 are summarized in Table 2 and show an acceptable agreement within approximately 30%<sup>2</sup>.

Table 2: Comparison of halo removal rates  $I_{\text{rel}}$  as obtained with SixTrack and Lifetrac for an e-beam current of  $I_e = 5$  A and DC and stochastic-amplitude (STA) mode.  $\Delta$  denotes the relative deviation of the SixTrack values from the Lifetrac values.

HEL mode	$Q'_{x,y}$	$I_{\text{oct}}$	$I_{\text{rel}} [\%]$		$\Delta$ [%]
			SixTrack	Lifetrac	
DC	3	0	13.6	19.9	32
	3	-450	10.9	17.0	35
	15	-550	17.4	24.0	28
	3	0	84.5	89.6	6
STA	3	-450	84.4	89.5	6

<sup>1</sup> The losses are normalized to the distribution after 10000 turns in order to account for a sufficient adjustment of the longitudinal distribution and any losses due to an initial mismatch of the distribution.

<sup>2</sup> A difference of this magnitude is to be expected due to the different models of the two simulation codes combined with the sensitivity of the particle trajectories to even small changes in case strong non-linearities like sextupoles, octupoles and also the HEL itself are present. However, studies are currently ongoing to better understand the origin of the differences and rule out any implementation errors.

### Dependence on e-Beam Current and Mode of Operation

As the maximum kick amplitude increases linearly with the e-beam current, the halo removal rates in general also increases with the same. The extent of the increase, however, depends on the operation mode and chosen scenario. As an example, the halo removal rates for DC operation, no octupoles and small chromaticity are listed in Table 3.

Table 3: Halo Removal Rate  $I_{\text{rel}}$  for Different e-Beam Currents  $I_e$  with  $Q'_{x,y}=3$  and no Octupoles

$I_e$ [A]	1.0	3.6	5.0	10.0
$I_{\text{rel}}$ [%]	1.2	9.9	18.0	45.2

A comparison of the different pulsing modes with and without octupoles is given in Fig. 4. In the stochastic-amplitude and stochastic-ONOFF mode, the halo is almost entirely removed within a few seconds and the modulation is the dominating loss mechanism as no difference is observed between with and without octupoles. For the resonant-turn mode the halo removal rate is smaller compared to the DC mode while with octupoles the it is larger for almost all pulsing patterns. The difference between the two modes is due to the fact that in stochastic modes all frequencies are excited while in resonant-turn mode only certain frequencies are excited and their amplitude also decreases with  $\frac{1}{n}$ .

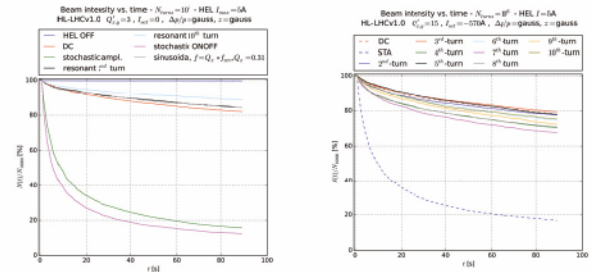


Figure 4: Surviving halo particles versus number of turns for different excitation modes of the HEL without (left) and with octupoles at  $I_{\text{oct}} = -570$  A (right).

### SUMMARY

The implementation of the HEL as a magnetic element in *SixTrack* was tested in a code benchmark with the tracking code *LifeTrac* for different e-lenses and HL-LHC parameters with a good accordance. This new implementation deploys HEL functionalities already tested in the past, in a way that is compatible with the standard *SixTrack* version for long-term simulation campaigns. The results of the HEL simulations for HL-LHC show that it is needed to operate the HEL either modulated or pulsed in order to reach fast and sufficient halo depletion in case of separated beams.

### ACKNOWLEDGMENT

We thank Dmitry Shatilov for his support with LifeTrac and R. Bruce, H. Garcia-Morales and D. Mirarchi for their help with SixTrack.

## REFERENCES

- [1] SixTrack 6D Tracking Code,  
<http://sixtrack.web.cern.ch/SixTrack/>
- [2] K. Sjobak *et al.*, “New features of the 2017 SixTrack release”, presented at IPAC’17, Copenhagen, Denmark, May 2017, paper THPAB047, this conference.
- [3] V. Previtali *et al.*, “Numerical simulations of a proposed hollow electron beam collimator for the LHC upgrade at CERN”, Fermilab, Batavia, USA, Rep. FERMILAB-TM-2560-APC, 2013.
- [4] C. Zanoni *et al.*, “Preliminary Mechanical Design Study of the Hollow Electron Lens for LHC”, presented at IPAC’17, Copenhagen, Denmark, May 2017, paper WEPVA117, this conference.
- [5] V. Shiltsev, “Electron Lenses for Super-Colliders”, Springer, 2016.
- [6] F. Schmidt, “SixTrack – User’s Reference Manual”,  
[http://sixtrack.web.cern.ch/SixTrack/doc/manual\\_dev/six.pdf](http://sixtrack.web.cern.ch/SixTrack/doc/manual_dev/six.pdf)
- [7] G. Stancari, “Calculation of the Transverse Kicks Generated by the Bends of a Hollow Electron Lens”, FERMILAB-FN-0972-APC.
- [8] I. Morozov *et al.*, “Simulation of Hollow Electron Beam Collimation in the Fermilab Tevatron Collider”, in *Proc. IPAC’12*, New Orleans, USA, May 2012, paper MOEPPB008, pp. 94 – 96.
- [9] M. Fitterer *et al.*, “Hollow Electron Beam Collimation for HL-LHC – Effects on the Beam Core”, presented at IPAC’17, Copenhagen, Denmark, May 2017, paper WEOBA2, this conference.
- [10] K. Sjobak *et al.*, “General functionality for turn-dependent element properties in SixTrack”, in *Proc. IPAC’15*, Richmond, VA, USA, May 2015, paper MOPJE069, pp. 468 – 471.
- [11] O. Bruening *et al.*, “Report from the Review Panel Needs for a hollow e-lens for the HL-LHC”, CERN, Geneva, Switzerland, October 2016.
- [12] D. Shatilov *et al.*, “Lifetrac code for the weak-strong simulation of the beam-beam effects in Tevatron”, in *Proc. PAC’05*, Knoxville, TN, USA, May 2005, paper TPAT084, pp. 4138 – 4140.
- [13] M. Fitterer *et al.*, “Simulation study of Hollow Electron Beam Collimation in HL-LHC”, Fermilab, Batavia, USA, Rep. FERMILAB-TM-2636-AD, October, 2016.
- [14] G. Stancari *et al.*, “Conceptual design of hollow electron lenses for beam halo control in the Large Hadron Collider”, FNAL, Batavia, IL, USA, Rep. FERMILAB-TM-2572-APC, CERN-ACC-2014-0248, Oct. 2014.